# Large Deflection Performance of Surface Micromachined Corrugated Diaphragms

C.J. van Mullem[1], K.J. Gabriel[2], H. Fujita

*Institute of Industrial Science, University of Tokyo, 7-22-1 Roppongi, Minato-ku, Tokyo 106, Japan.*

[1] MESA Research Institute, University of Twente, The Netherlands.
[2] AT&T Bell Laboratories, Holmdel, U.S.A.

## Abstract

Large deflection performance of corrugated diaphragms were measured and modelled for their dependence on diaphragm geometries and corrugation parameters. Corrugated polyimide diaphragms of various diameters, corrugation frequencies, and thickness were fabricated using a surface micromachining technique. Current models correctly described the observed increase in deflection from corrugated diaphragms compared to deflections from flat diaphragms at equivalent loads. In addition, the models are extended with the definition of the transition deflection, $y_t$, which delineates the transition between the small and large deflection regions. The range of corrugation quality factors available in surface micromachined diaphragms is determined and predicted load-deflection curves are compared to measurements. Although corrugation spatial frequency is predicted to have a small effect on diaphragm performance, results show significant large deflection behaviour difference between diaphragms of similar corrugation quality factors but different corrugation spatial frequencies. Large deflection behaviour of FEM simulations shows a similar effect due to corrugation frequency.

## Introduction

Diaphragms are an integral part of many solid-state sensors and corrugation techniques have been developed to increase the linear portion of the load-deflection behaviour of such diaphragms [1,2,3]. In IC-based actuator applications, corrugated diaphragms can provide larger deflections than flat diaphragms for equivalent loads and can lead to improvements in the performance of valves, pumps and thin-film mirrors. In addition, corrugated zones or diaphragms can be used to mechanically decouple a micromechanical sensor from its package [4,5].

Previous work on corrugated diaphragms has been concerned with extending the linear portion of the load-deflection behaviour to improve sensor performance and extend the range of sensor operation. In this study however, we focus on the load-deflection behaviour of corrugated diaphragms designed to operate in the large deflection (deflections many times greater than the diaphragm thickness) region appropriate for actuator applications. We first describe the modelling of corrugated diaphragms, including the definition of a transition deflection, $y_t$, which delineates the transition between the small and large deflection regions. Next, the surface-micromachining fabrication sequence used to realize the polyimide diaphragms is outlined. The load-deflection measurement station is then described and typical load-deflection curves are presented. Finally, predicted and obtained results are compared and the effect of corrugations on load-deflection behaviour is discussed.

## Modelling of Corrugated Diaphragms

The load-deflection relation of a flat, clamped circular diaphragm is given by [1]:

$$\frac{Pa^4}{Eh^4} = \frac{16}{3(1-\nu^2)}\left(\frac{y}{h}\right) + \frac{7-\nu}{3(1-\nu)}\left(\frac{y}{h}\right)^3 \qquad (1)$$

where $P$ is the applied pressure, $a$ is the diaphragm radius, $E$ the Young's modulus, $h$ the diaphragm thickness, $\nu$ the Poisson's ratio and $y$ the center deflection of the diaphragm. The deflection range is divided into two regions: a small deflection region (deflections less than half the diaphragm thickness) described by the linear term in Equation 1, and a large deflection region described by the non-linear, cubic term in Equation 1. For our purpose, the large deflection region is the one of interest. In the models, the intrinsic stress due to the fabrication process of the diaphragm has not been taken into account since we are primarily concerned with the non-linear, large deflection behaviour of the diaphragm [6].

Introducing corrugations into a diaphragm alter the coefficients of the linear and cubic terms in Equation 1, increasing both: (1) the transition deflection, $y_t$, below which deflections remain linear and (2) the deflection of corrugated diaphragms in the large deflection region for equivalent loads. The coefficients are dependent on the diaphragm geometry and the corrugation parameters, with the load-deflection relation given by [1]:

$$\frac{Pa^4}{Eh^4} = A_p\left(\frac{y}{h}\right) + B_p\left(\frac{y}{h}\right)^3 \qquad (2)$$

with

$$A_p = \frac{2(q+2)(q+1)}{3(1-(\nu/q)^2)}$$

$$B_p = \frac{32}{q^2-9}\left(\frac{1}{6} - \frac{3-\nu}{(q-\nu)(q+3)}\right)$$

where $q$ is the corrugation quality factor. For sinusoidal corrugation profiles, the quality factor is defined as:

$$q^2 = \frac{s}{l}\left(1 + 1.5\left(\frac{H}{h}\right)^2\right) \qquad (3)$$

with $H$ being the corrugation depth, $s$ the corrugation arc length and $l$ the corrugation spatial period. The quality factor of a flat diaphragm is 1 and for the surface micromachined diaphragms considered in this study, the maximum quality factor is near 10 because of limitations in the minimum diaphragm thickness and in the vertical dimensions of the fabrication process. Although our fabrication process results in

91CH2817-5/91/0000-1014$01.00 © 1991IEEE

rectangular corrugation profiles, the specific profile shape has little influence on the quality factor [1]. Note that in the above model, the corrugation spatial period (or corrugation frequency) should have little effect on deflection performance since for shallow corrugation ($H << l$), $s/l$ is nearly unity.

In Figure 1, the simulated load-deflection characteristics of three diaphragms are given: one flat and two corrugated with a $q$ of 4 and 8. The parameters for all three diaphragms are $a$ = 0.5 mm, $h$ = 1 μm and $E$ = 3 GPa (a polyimide diaphragm). This figure clearly indicates the effects of introducing corrugations into the diaphragm. In the small deflection region, the increase in the linear portion of the load-deflection behaviour for the corrugated diaphragm is also illustrated. Note that increasing the linearity by introducing corrugations causes a concomitant increase in the load necessary to obtain an equivalent deflection in a flat diaphragm. In some sensor applications (for example a low-pressure sensor with capacitive deflection sensing), introducing corrugations may be a *disadvantage* since the improved linearity is gained at the expense of reduced sensitivity in the small deflection region.

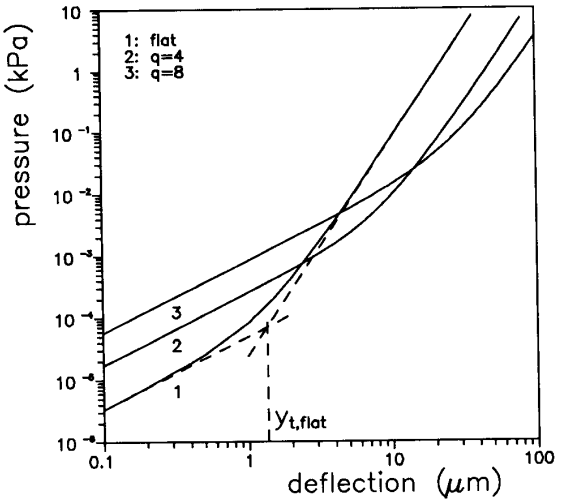


*Figure 1 Load-deflection characteristics of flat and corrugated diaphragms.*

The transition from the small deflection region to the large deflection region is delineated by the transition deflection, $y_t$, which we define as the deflection where the contribution of the linear and non-linear terms are equivalent. From Equation 2 we obtain:

$$y_t = h\left(\frac{A_p}{B_p}\right)^{1/2} \tag{4}$$

Substituting $y_t$ into Equation 2, we can also calculate a corresponding transition load or pressure, $P_t$. In Figure 2 the normalized transition deflection, $y_n$ ($y_t/y_{t,flat}$) and $P_n$ ($P_t/P_{t,flat}$) are given as a function of the quality factor. As seen in Figure 2, both $y_n$ and $P_n$ increase rapidly with increasing $q$. Note that for a $q$ of 10, $P_n$ is approximately 500, an increases in the transition load of more than two orders of magnitude. For actuator applications designed for use in the large deflection

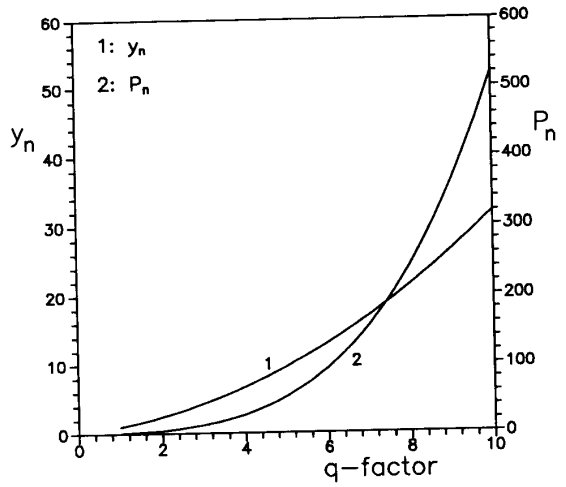


*Figure 2 The normalized deflection and load as function of the q-factor.*

region, the increase in the transition deflection and load due to adding corrugations to the diaphragms has to be considered.

## Fabrication Process of Corrugated Diaphragms

Methods for the fabrication of corrugated diaphragms are numerous. One recent method is based on selective etching of silicon using high-boron doping [2]. However, to provide greater design flexibility and future integration with other surface micromachined components, we chose to fabricate thin-film corrugated diaphragms using a sacrificial layer etching technique. The sacrificial layer defines both the corrugation profile and the diameter of the diaphragm. The entire fabrication sequence consists of three photolithographic steps and is outlined in Figure 3.

The first step of the fabrication process is the anisotropic etch of the access holes from the back of the silicon wafer, resulting in a thin silicon diaphragm. Later on in the process, these access holes are completely etched through to provide etchant access to the sacrificial material and used as input ports for the applied pressure to the diaphragm. Next, the sacrificial material, aluminum, is deposited on the front side of the wafer, the thickness of the aluminum defining the maximum corrugation depth. A partial time etch of the aluminum layer is performed which defines the corrugation profile and a subsequent full etch defines the diaphragm size. The third step in the fabrication is the spin-on deposition of a polyimide layer (DuPont PI-2610) as the thin-film diaphragm [6]. Finally, the remaining silicon in the access holes is removed using RIE and the diaphragms are released by wet-etching the sacrificial, aluminum layer in a commercial etchant.

The success of the final release step is critically dependent on the size of the access holes relative to the diaphragm diameter. Optimal results were obtained when access holes were at least half the diameter of the diaphragm. For some of the larger diameter diaphragms, etches of up to 24 hours were required to completely release the diaphragms. Flat diaphragms of similar dimensions were also fabricated on the same wafer to provide control structures for comparison with corrugated diaphragms.

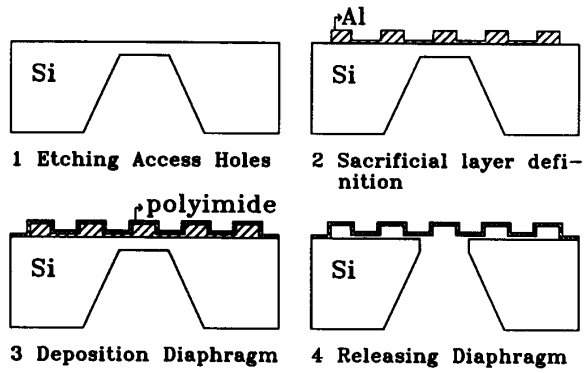


*Figure 3 Schematic view of the fabrication process of corrugated diaphragms*

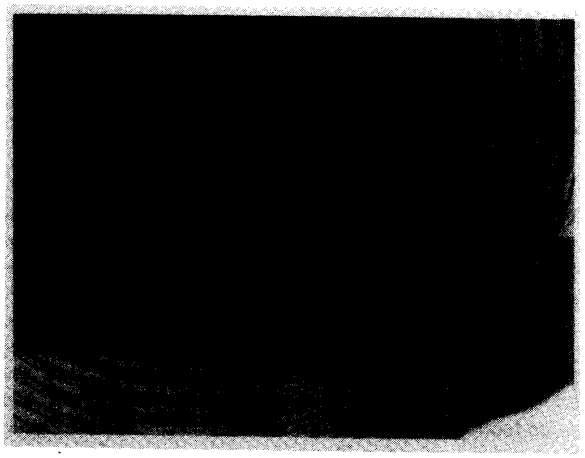

*Figure 4 Corrugated diaphragm, corrugation period is 50 μm.*

Figure 4 is a photograph of a circular, corrugated diaphragm with a radius of 1 mm and a corrugation period of 50 μm. The dark square area is a part of the access hole etched from the back side of the wafer. The corrugation profile differs slightly from a rectangular profile due to the under etching of the corrugation mask and also because of the relative ratio of the diaphragm thickness and the corrugation period.

In a later version of the fabrication process, the definition of the sacrificial layer is modified. The first etch of the sacrificial layer still defines the corrugation profile, but is now a complete etch rather than a partial etch. Thus the corrugation depth is now controlled by the deposition thickness instead of the timed etch. The next step is a second deposition of the sacrificial material which defines the diaphragm size without affecting the corrugation depth. With this modification, all thicknesses are deposition controlled providing more precise control of the corrugation depth.

## Load-Deflection Performance of Corrugated Diaphragms

The measurements of the load-deflection curves are performed with an optical measurement set-up using a z-stage calibrated optical microscope [7]. In Figure 5, the principal set-up is

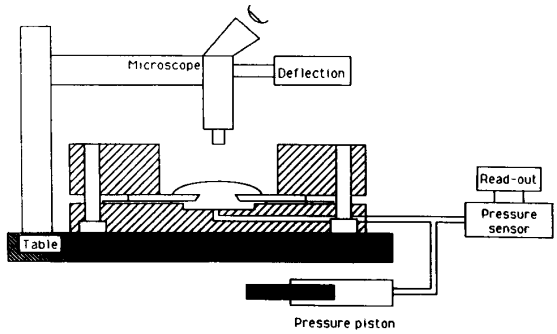


*Figure 5 The load-deflection measurement set-up.*

drawn. The silicon substrate with a flat or corrugated diaphragm is clamped to a pressure chamber which is connected to a calibrated solid-state pressure sensor. A differential pressure applied to the diaphragm causes it to deflect upward. By successively focussing the microscope at increasing pressure values, a load-deflection curve is obtained.

In Figure 6, the measured load-deflection characteristics for flat and corrugated polyimide diaphragms are given. The diaphragm thickness is 2.5 μm and the radius is 1 mm. The corrugation depth is 2 μm and the corrugation period is 200 and 50 μm. These dimensions result in a $q$ of 1.4 for the two corrugated diaphragms. As expected, for equivalent loads, the deflections of the corrugated diaphragms in the large deflection region are greater than the deflection of the flat diaphragm. The transition load and deflection increase for the corrugated diaphragms compared to the flat diaphragm. Surprisingly, although the two corrugated diaphragms had identical $q$ factors and our model predicts little effect from the corrugation frequency, the higher corrugation frequency diaphragm exhibited larger deflections at the same load.

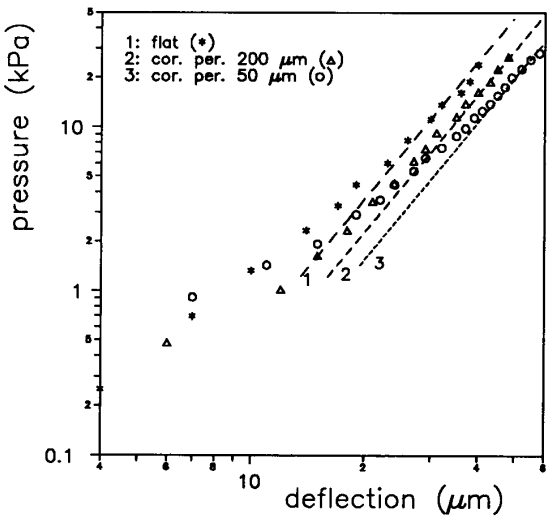


*Figure 6 Measured load-deflection characteristics for flat and corrugated diaphragms.*

The dashed lines in Figure 6 are curve fits in the large deflection region of the load-deflection measurements. As expected from the modelling, a cubic function describes the observed deflections for both the flat and corrugated diaphragms. The decrease in the cubic coefficient ($B_p$) of the corrugated diaphragms relative to the coefficient of the flat diaphragm is in good agreement with the modelling. Predicted values for the ratio of $B_{p,flat}/B_{p,cor}$ for a $q$ of 1.4 is approximately 1.8. The obtained ratios for the 200 μm and 50 μm corrugation period diaphragms are 1.46 and 2.20 respectively. However, the predicted values of $B_p$ for both the flat and corrugated diaphragms were less than the values obtained from the measurements. One explanation may be the change in the Young's modulus of the polyimide due to the relatively long etch time necessary for the removal of the sacrificial layer.

To investigate the influence of the corrugation frequency on the large deflection behaviour of corrugated diaphragms with high $q$-factors and rectangular profile, finite element modelling was performed using COSMOS/M. One flat and two corrugated diaphragms were modelled with $E$ = 3 GPa, $a$ = 0.5 mm, $h$ = 2 μm and $H$ = 8 μm. The results are given in Figure 7 with the solid line the model for a flat diaphragm and the dashed lines curve fits for the linear and non-linear region of the corrugated diaphragms. The FEM simulations of the large deflection behaviour result in a qualitative match with the measured behaviour of corrugated diaphragms with different corrugation frequencies. Refinements on the existing model are necessary to incorporate the effect of the corrugation frequency.

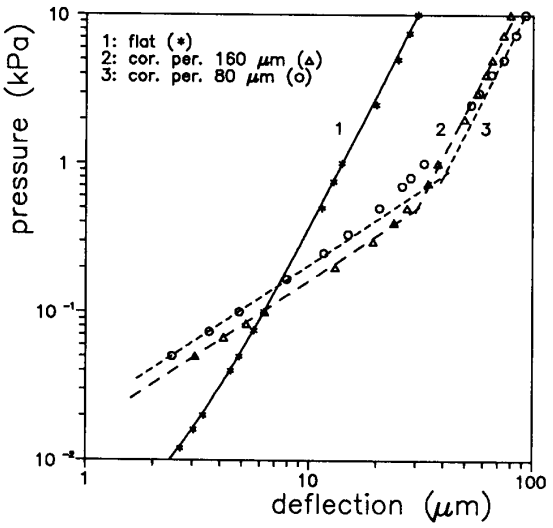


*Figure 7 FEM simulations of circular flat and rectangular corrugated diaphragms.*

## Summary

Large deflection performance of diaphragms is strongly influenced by the introduction of corrugations into the diaphragm. In the large deflection region and at equivalent loads, deflections of corrugated diaphragms are increased compared to the deflections of flat diaphragms. In the small deflection region, the introduction of corrugations extends the linear portion of the load-deflection behaviour, but at the expense of increased load for an equivalent deflection in a flat diaphragm.

Surface micromachining with polyimide as the structural material and aluminum as the sacrificial material was used to fabricate thin-film corrugated diaphragms. Release of the diaphragm from anisotropically etched access holes in the back was found depend critically on the size of the access holes relative to the diaphragm diameter. Optimal results were obtained when access holes were at least half the diameter of the diaphragm.

The load-deflection characteristics in the large deflection region show the predicted increase in deflection for corrugated diaphragms. However, while the ratio of the cubic coefficients, $B_{p,flat}/B_{p,cor}$, are in agreement with the model, the individual $B_p$ values are underestimated by the model. Finally, although the model predicts little effect of corrugation frequency on load-deflection behaviour, we observe significant differences in the measured large deflection behaviour between two corrugated diaphragms of similar dimensions and $q$ but different corrugation frequencies. FEM simulations show a similar effect due to corrugation frequency for diaphragms with a high $q$-factor. Refinements on the existing model are necessary to incorporate the effect of the corrugation frequency.

## Acknowledgement

One of the authors (C.J. van Mullem) was jointly supported by the Institute of Industrial Science, University of Tokyo and the Dutch Foundation for Fundamental Research on Matter (FOM) during his stay as visiting researcher at the Institute of Industrial Science.

## References

[1] M. Di Giovanni, Flat and corrugated diaphragm design handbook, Marcel Dekker Inc., New York, 1982.

[2] J.H. Jerman, "The fabrication and use of micromachined corrugated silicon diaphragms", *Sensors and Actuators*, vol. A21-A23, 1990, pg. 988-992.

[3] S. Timoshenko and S. Woinowsky-Krieger, Theory of plates and shells, McGraw-Hill Book Co., New York, 1959, pg. 404.

[4] V.L. Spiering, S. Bouwstra, M. Elwenspoek, J.H.J. Fluitman, "On-chip decoupling zone for package-stress reduction", presented at *Transducers'91*, San Francisco, U.S.A., 1991.

[5] H.L. Offereins and H. Sandmaier, "Novel stress free assembly technique for micromechanical devices", in *Proc. of the Conference Micro System Technologies'90*, Berlin, Germany, Sept. 1990.

[6] M.Mehregany, "Application of micromachined structures to the study of mechanical properties and adhesion of thin-films", Msc report, MIT, 1986, pg. 51-108.

[7] J.A. Walker, K.J. Gabriel, M. Mehregany, "Mechanical integrity of polysilicon films exposed to hydrofluoric acid solutions", *Technical Digest of IEEE MEMS Workshop*, Napa Valley, U.S.A., 1990, pg. 56-60.